Matakatsu et al., https://doi.org/10.1083/jcb.201609094

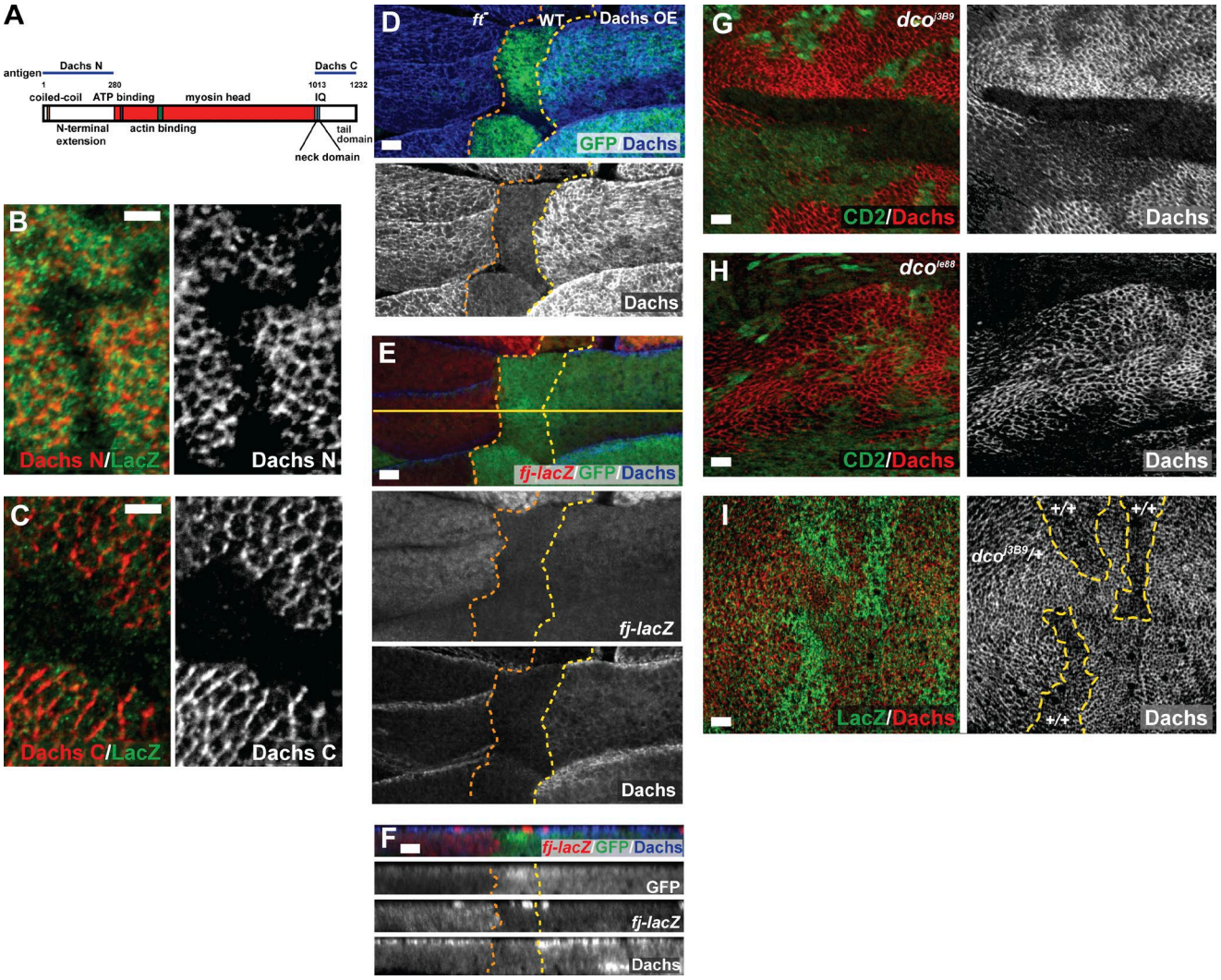

Figure S1. **Specificity of anti-Dachs antibodies and Dachs localization in *ft* mutant cells when ectopically expressed and in strong *dco* alleles.** Related to Fig. 1. (A) Diagram of Dachs structure, with major domains and regions used as antigens for making antisera indicated. The myosin head domain is indicated in red. The blue lines show Dachs N and C antigens. (B and C) Staining of *dachs* null clones demonstrates that the antisera specifically recognize Dachs in tissues. Dachs staining with anti-Dachs antibodies (B for anti-Dachs N and C for anti-Dachs C) is lost in $dachs^{GC13}$ mitotic clones. Mutant clones are marked by the absence of anti-LacZ staining (green in B and C). (D–F) *ft* mutant mitotic clones (GFP negative) were induced in wing imaginal discs in the background of *hh-Gal4*–driven UAS-Dachs expressed in the posterior compartment (yellow dotted lines). (D) In the apical region, overall Dachs staining appears higher in cells ectopically expressing Dachs than in *ft* mutant cells. (E) *fj-lacZ* is up-regulated in *ft* mutant cells and only weakly up-regulated in cells ectopically expressing Dachs. (F) Optical cross sections at the yellow line in E. Ectopically expressed Dachs accumulates at the AJR and in the basal cytoplasm. (G–H) Anti-Dachs staining in dco^{i3B9} (G) and dco^{le88} (H) mutant cells. Mutant clones were induced in a *Minute* background and marked by the absence of CD2 staining. Anti-Dachs staining at the AJR is elevated in *dco* mutant clones. (I) Comparison of Dachs staining between wild-type (+/+) and dco^{i3B9}/+ cells. The mitotic clones are marked by the absence of anti-LacZ staining. dco^{i3B9} homozygous clones are eliminated from the imaginal epithelium in the absence of a *Minute* mutation to confer a growth advantage. The boundary between wild-type and dco^{i3B9}/+ cells is marked with yellow dotted lines. The intensity of anti-Dachs staining in wild-type cells (+/+) is lower than that of dco^{i3B9}/+ cells. Bars, 5 µm.

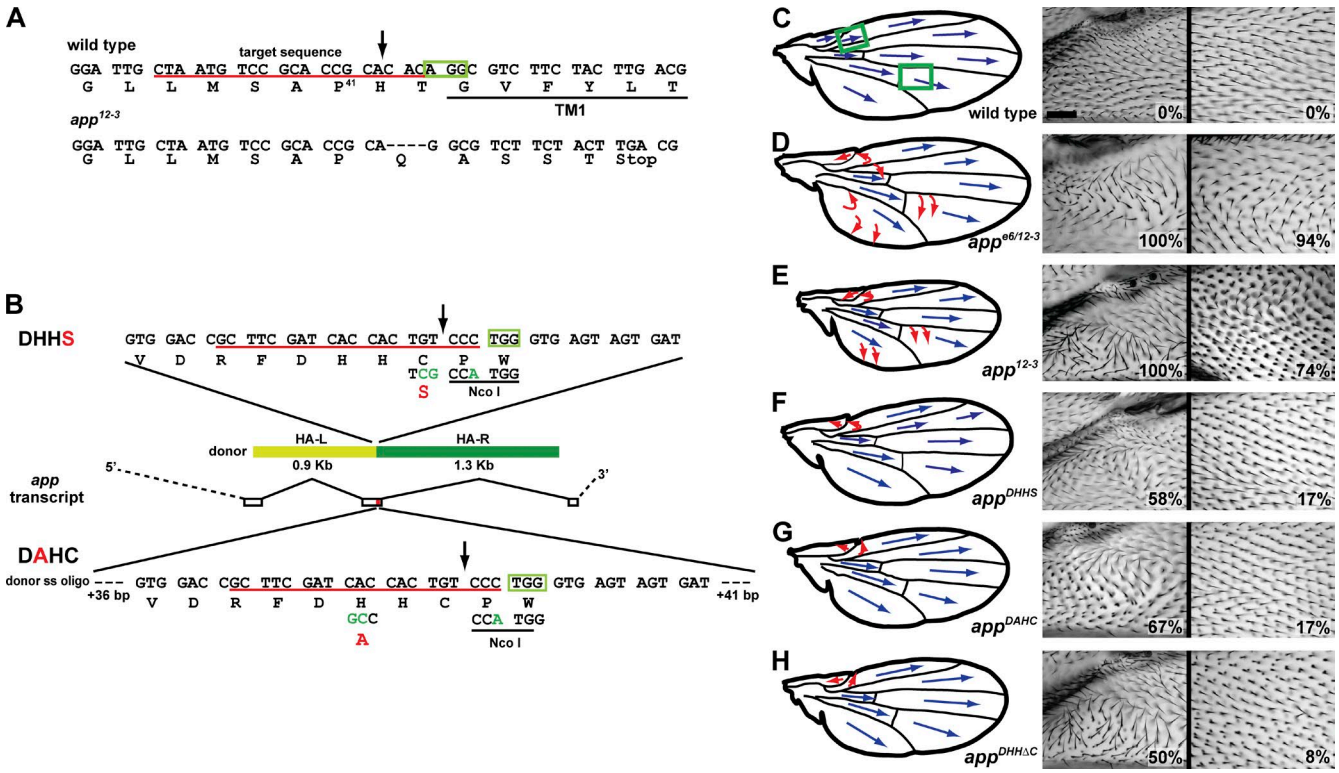

Figure S2. **CRISPR-Cas9–induced *app* alleles and their planar cell polarity (PCP) phenotypes.** Related to Fig. 2. (A) The molecular lesion associated with *app*$^{12\text{-}3}$. A 4-bp deletion near the N terminus of App creates a frameshift that leads to a premature stop codon. TM1, first transmembrane domain. (B) CRISPR-Cas9–induced mutations in the DHHC domain. Target sequence, donor DNA, and restriction sites are shown. HA-L, left homology arm; HA-R, right homology arm. (C–H) PCP phenotypes in the wing. PCP in wild-type (C) or *app* (D–H; genotypes as indicated) mutant wings. Blue arrows, normal PCP; red arrows, abnormal PCP. The details of hair polarity in adult wings from proximal (middle) and distal (right) regions correspond to the green boxes in C. The overall frequency of PCP defects is shown in each photo (n > 20 for each genotype). Bar, 100 µm.

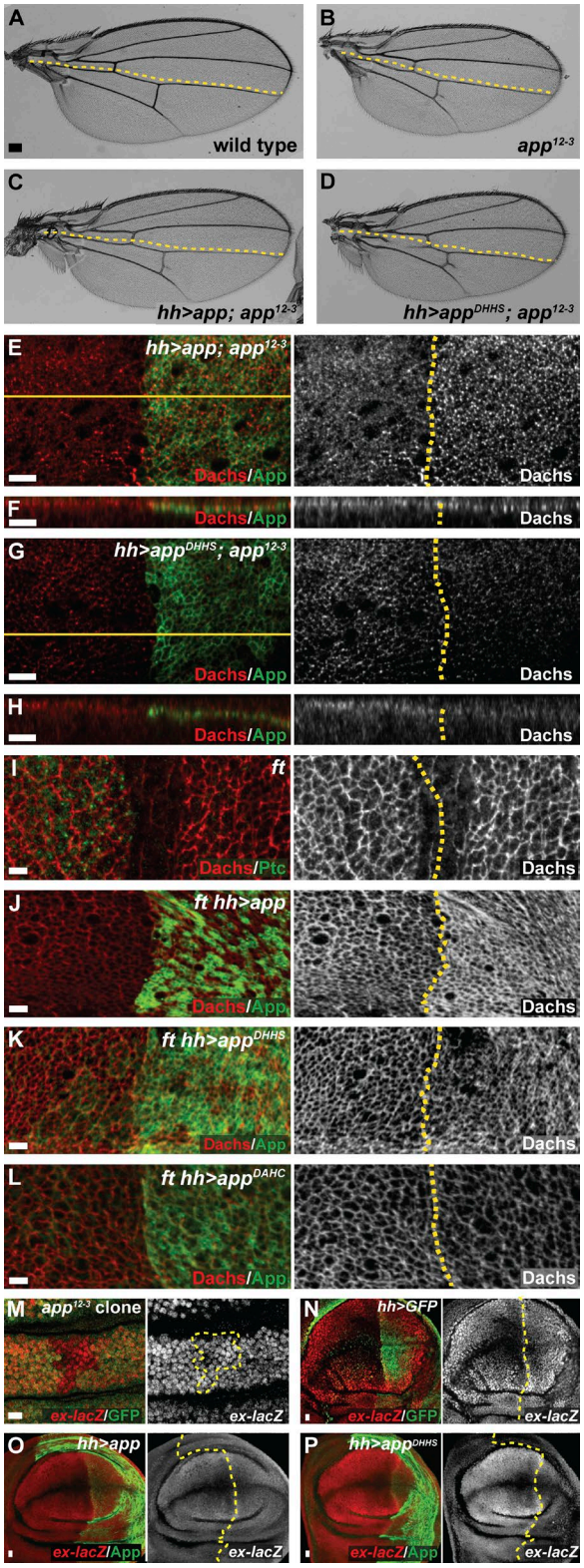

Figure S3. **Effects of ectopic expression of wild-type and mutant alleles of *app* on wing size, Dachs accumulation at the AJR, and the *ex-lacZ* Hippo reporter.** Related to Fig. 2. (A–D) Representative wings from wild-type (A), *app*$^{12\text{-}3}$ (B), *UAS-app; hh-gal4 app*$^{12\text{-}3}$*/app*$^{12\text{-}3}$ (C), and *UAS-app*^{DHHS}*; hh-gal4 app*$^{12\text{-}3}$*/app*$^{12\text{-}3}$ (D) animals. Ectopic expression of wild-type App rescued growth in posterior compartment (C), whereas expression of App^{DHHS} reduced growth (D). (E and F) *hh-gal4*–driven wild-type App expression rescued Dachs localization at the AJR. (G and H) *hh-gal4*–driven App^{DHHS} expression resulted in decreased Dachs localization at the AJR. (I) Dachs staining in a *ft* mutant wing epithelium. Dachs level is similar across the anterior–posterior boundary, which is marked with a yellow dotted line in all panels. (J) Ectopic wild-type App expression caused increased Dachs accumulation at the AJR in *ft* mutant cells. (K and L) Ectopically expressed App^{DHHS} (K) or App^{DAHC} (L) has little or no effect on Dachs. (M) Expression of *ex-lacZ* was unaffected in *app*$^{12\text{-}3}$ mitotic clones. (N) Wild-type *ex-lacZ* expression. (O and P) Ectopic expression of wild-type App had no effect on *ex-lacZ* expression (O), whereas expression of App^{DHHS} led to down-regulation of *ex-lacZ* expression (P). Bars, 5 µm.

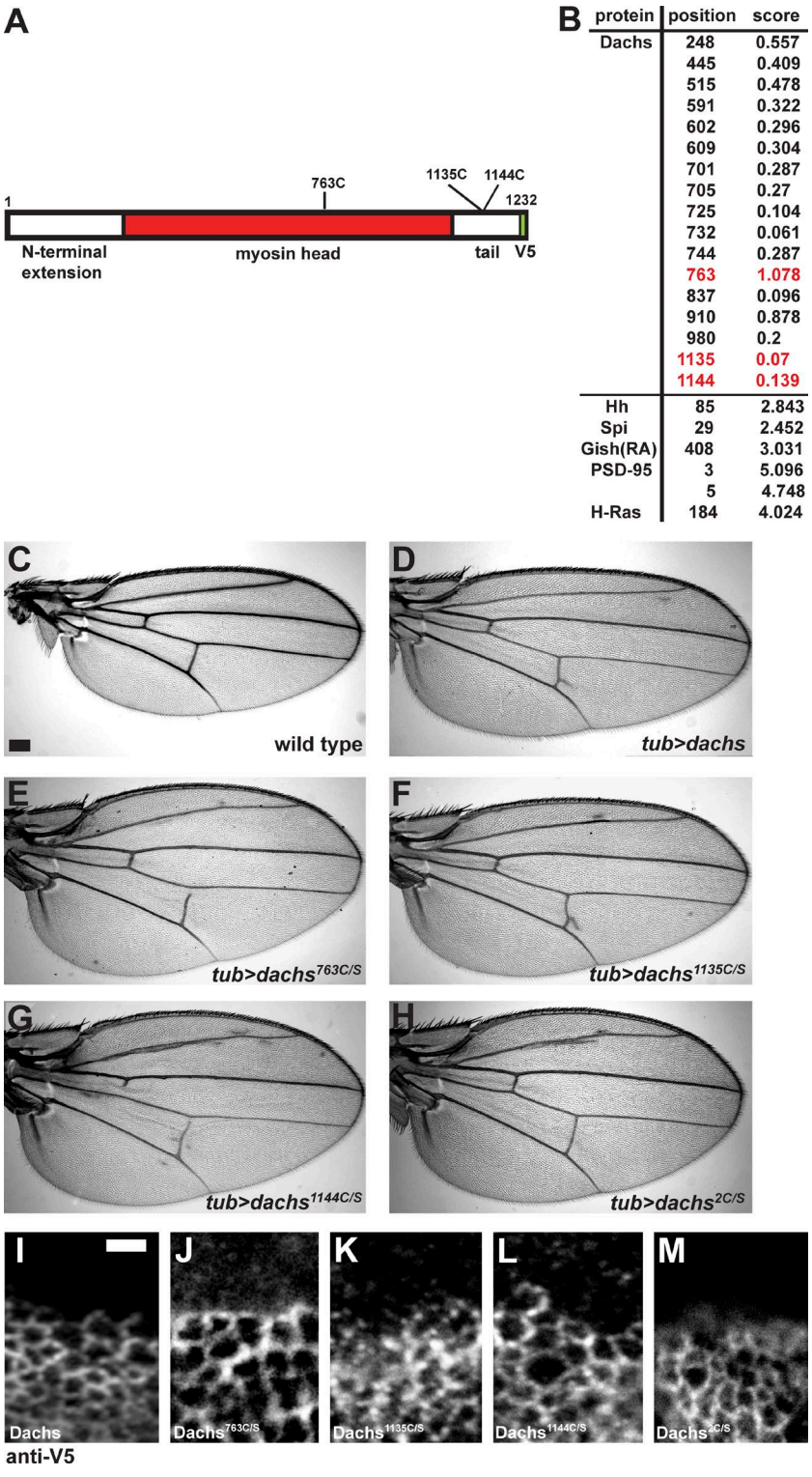

Figure S4. **Mutation of possible palmitoylation sites in Dachs does not significantly affect its function.** Related to Fig. 3. (A) The structure of Dachs indicating Cys residues mutated to Ser for these experiments. (B) The predicted palmitoylation site scores using CSS-Palm 2.0 in Dachs, Hedgehog (Hh), Spitz (Spi), Gilgamesh (Gish), PSD-95, and H-Ras. Dachs positions in red indicate substituted cysteines. (C–H) Wings of the indicated genotypes showing the effects of ectopic expression of different Cys mutants. All promoted overgrowth similarly to wild-type Dachs. (I–M) Cys substitution mutants in Dachs do not affect its localization at the AJR (anti-V5 staining). Bars: (C) 100 µm; (I) 5 µm.

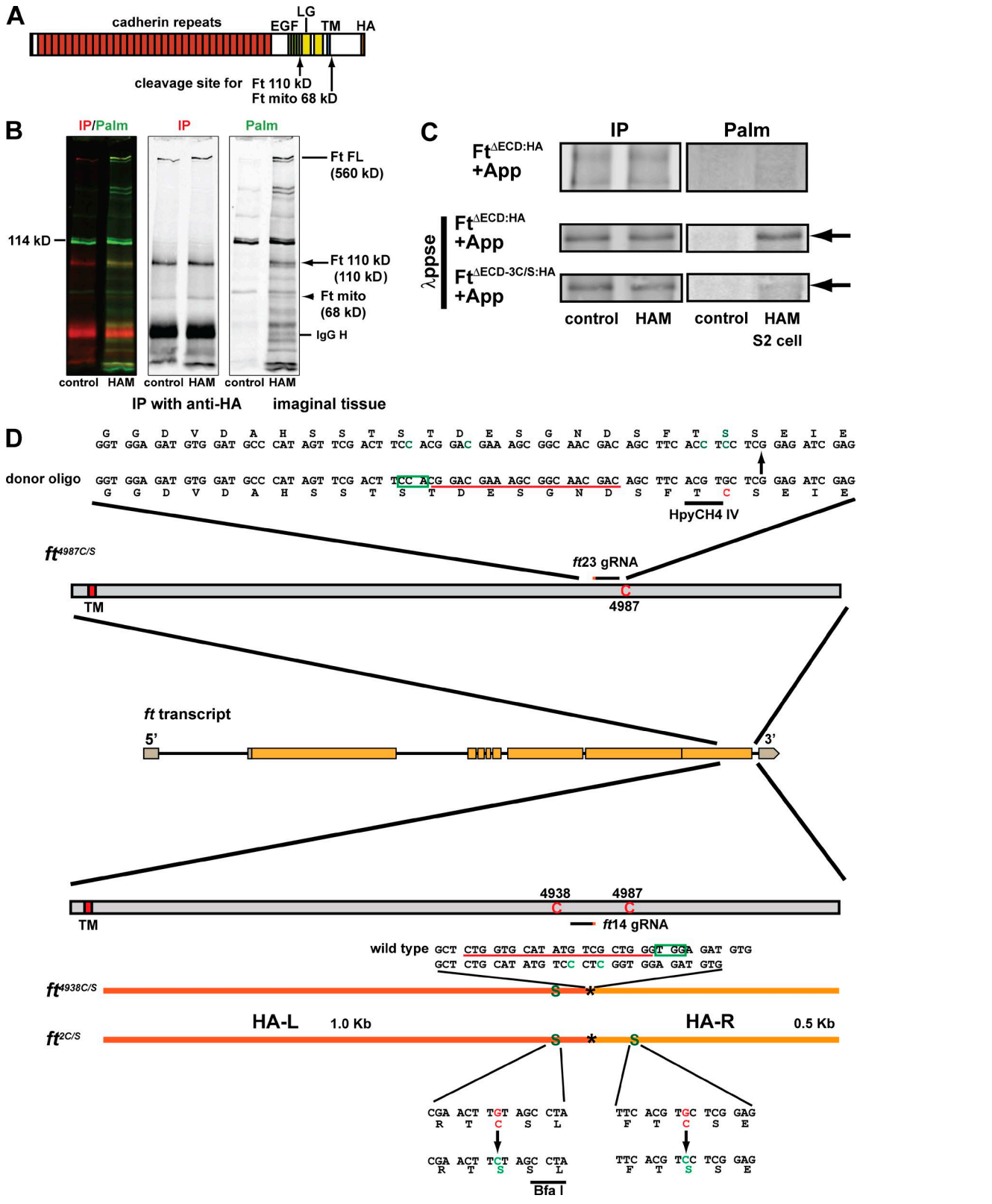

Figure S5. **Palmitoylation of Ft fragments and mutation of intracellular Cys residues in *ft* using CRISPR-Cas9.** Related to Fig. 4. (A) The structure of Ft:HA indicating major domains. Ft is cleaved and produces 110- and 68-kD (Ft mito) fragments (arrows) at the C-terminal end. (B) Palmitoylation of Ft fragments in vivo. Ft:HA was expressed using *da-gal4*. The merged image (left), anti-HA staining (IP; middle), and palmitoylation (Palm; right) are shown. Full-length Ft (Ft FL), Ft 110-kD, and Ft mito are all palmitoylated. (C) Without phosphatase treatment, $Ft^{\Delta ECD}$ expressed in S2 cells migrated as a smeared band positive for palmitoylation (top). This reduced to a single band after lambda phosphatase treatment (middle; arrow indicates $Ft^{\Delta ECD}$). Substitution of all three intracellular cysteines strongly reduced the palmitoylation signal (bottom). (D) Target sequence, donor DNA, and restriction site are shown. Asterisk indicates mutation introduced in the PAM sequence to prevent cleavage by the *ft*14 guide RNA (gRNA).

Table S1. **Viability of *app*, *dco*, and double mutant allele combinations**

	Wild type	dco^3	$app^{12\text{-}3}$	app^{DHHS}	$dco^3\ app^{12\text{-}3}$	$dco^3\ app^{DHHS}$
expected	125	289	226	128.5	185.5	280.5
observed	118	0	128	115	89	131
% viability	94.4	0	56.6	89.5	48	46.7